Supporting Information

Stabilisation of high-valent Cu^{3+} in a Keggin-type polyoxometalate

Xiang Li,[a] Yuanhang Ren,[a] Zhewei Weng,[a] Bin Yue [a*] and Heyong He [a*]

The characterisation details, ESI-MS results, IR spectra and TG curve of 1-Cs, XPS spectra of 1-Cs and 2-Cs are provided here.

General characterisation methods

XRD patterns were recorded on a Bruker D2 Advance diffractometer with Cu *Kα* radiation (λ = 1.5418 Å) operated at 10 mA and 30 kV. The scanning rate was $3°\cdot min^{-1}$ from 5 to 90°. The FT-IR spectra were recorded in the range of 4000-500 cm^{-1} with a Nicolet Nexus 470 FTIR spectrometer using KBr pellets. Elemental analysis was performed on a Thermo Elemental IRIS Intrepid ICP atomic emission spectrometer. XPS measurements were conducted in the range of 0-1100 eV under a pressure of 1.0×10^{-6} Pa on a PerkinElmer PHI 5000C ESCA X-ray photoelectron spectrometer using Mg *Kα* radiation (1253.6 eV). Calibration was conducted with the contaminant carbon (C 1s = 284.6 eV). UV-Vis diffuse reflectance spectra were recorded with a Lambda 650S UV-Vis spectrometer. Thermogravimetric analysis was performed on a Mettler Toledo TGA/DSC 3+ thermogravimetric analyser in a range of 40~700 ºC with a temperature rising rate of 10 ºC/min.

Magic angle spinning solid-state nuclear magnetic resonance spectroscopy (MAS NMR)

The ^{31}P MAS NMR spectra were recorded on a Bruker AVANCE III 400WB spectrometer at 162.1 MHz with a spinning rate of 12 kHz and 85% H_3PO_4 as the standard. The pulse width was 1.1 μs and the relaxation delay was 15 s. The sample was dried *in vacuo* and then transferred into a Bruker 4 mm zirconia rotor under nitrogen atmosphere.

Electrospray ionisation mass spectrometry

The mass spectrometry was conducted on a Bruker MicrOTOF II mass spectrometry in the m/z range of 1200-6000 with a capillary voltage of 4000 V and an electrospray ionisation (ESI) source. The mode was negative ion. The nebuliser pressure was 1.0 bar and the dry heater temperature was 180 ºC with a dry gas flow of $4.0\ L\cdot min^{-1}$.

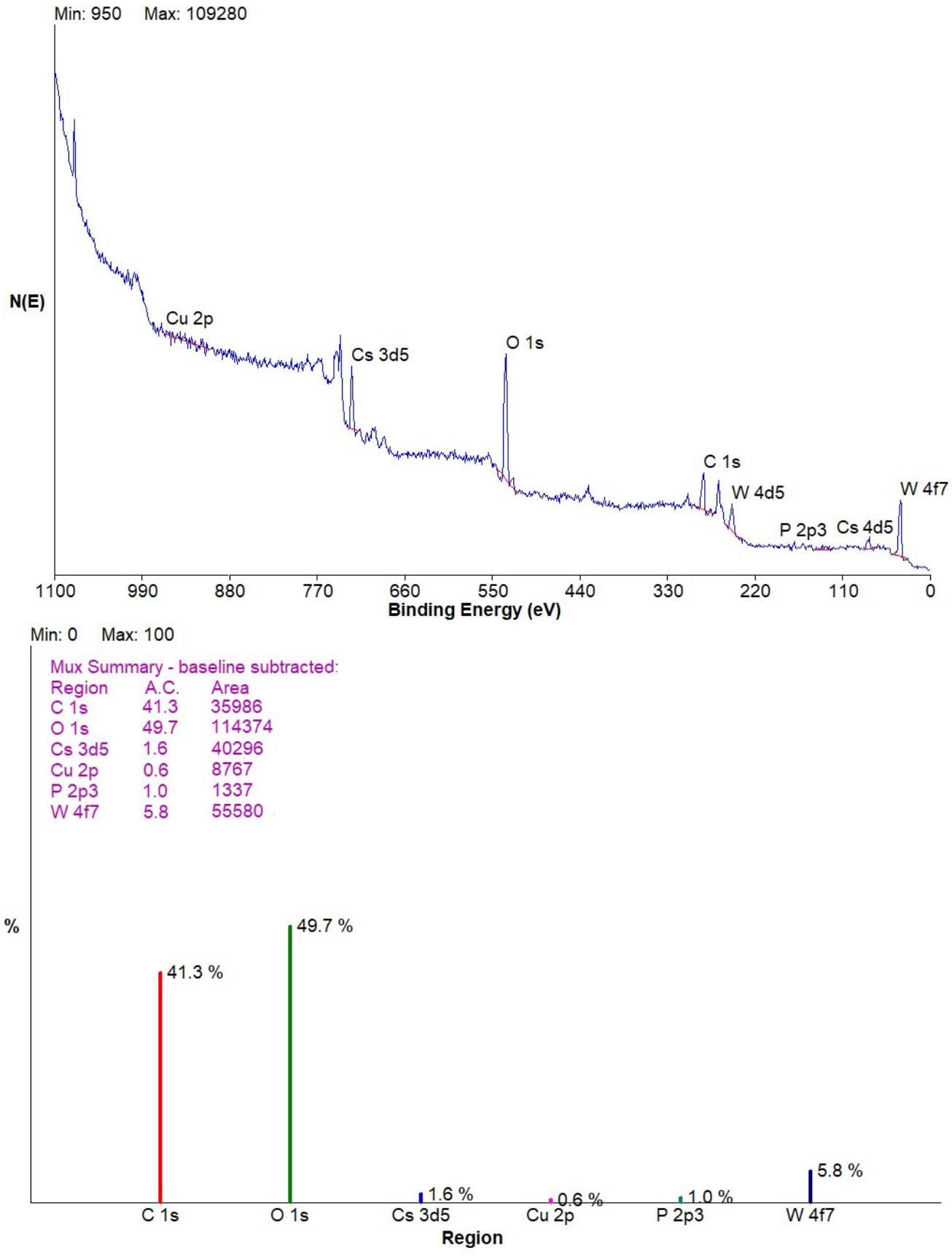

Fig. S1 XPS survey spectrum and the corresponding quantitative result of **1-Cs.**

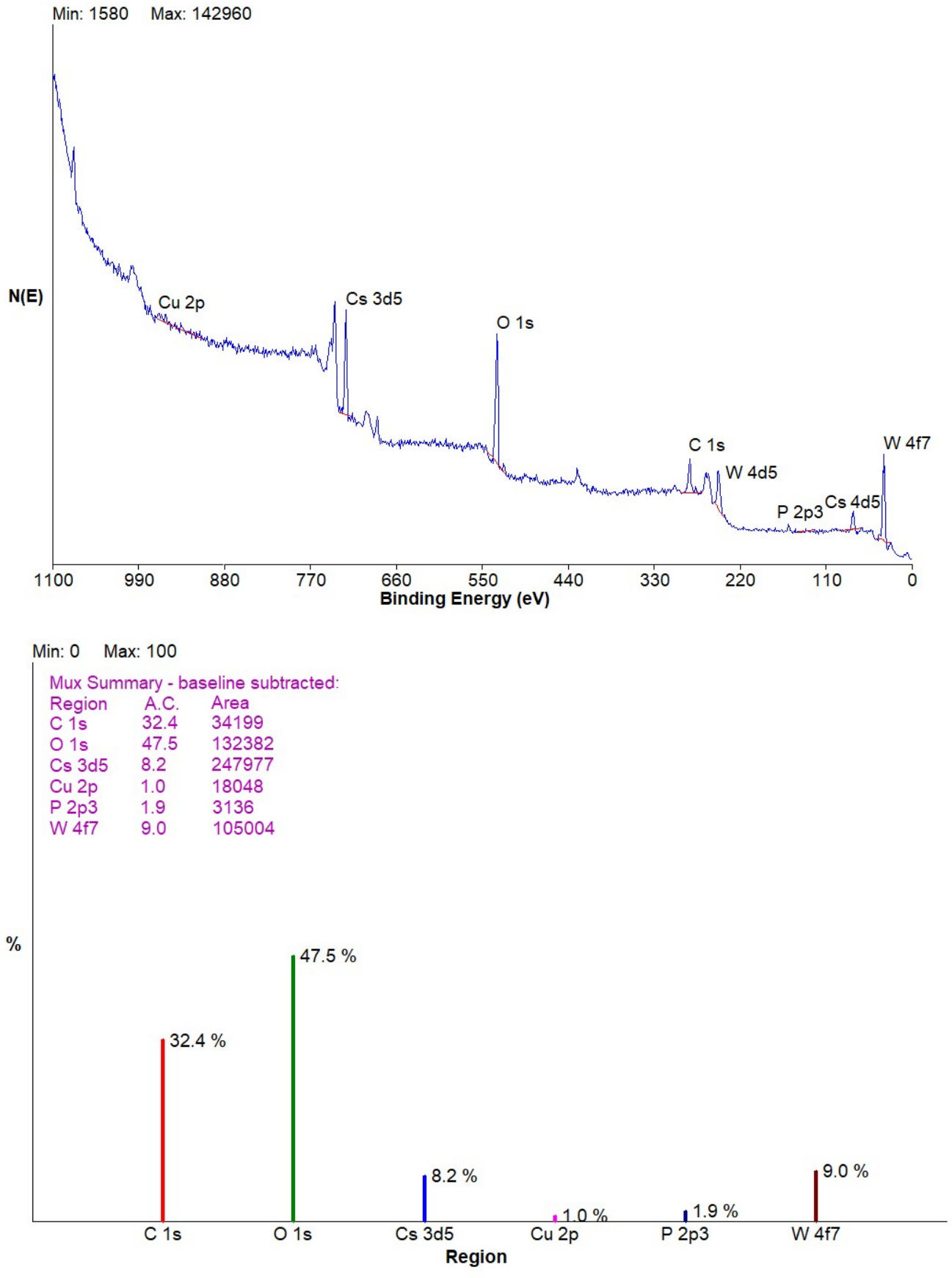

Fig. S2 XPS survey spectrum and the corresponding quantitative result of **2-Cs.**

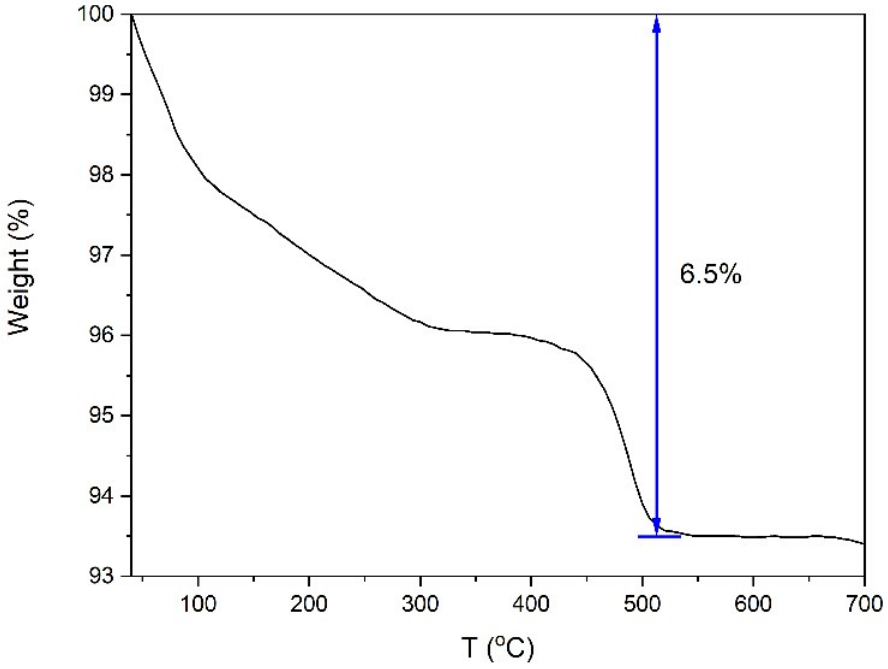

Fig. S3 TG curve of **1-Cs**.

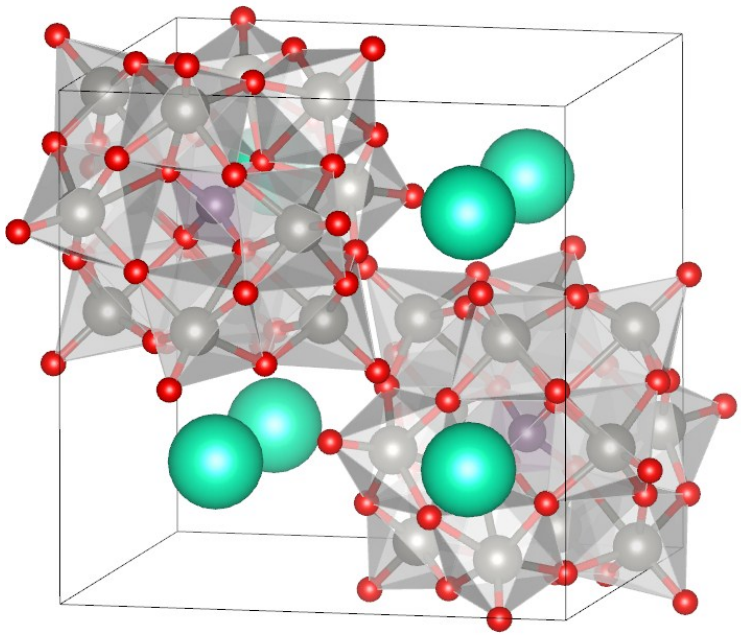

Fig. S4 Crystal structure of **3-Cs**.[A1,A2] The structure of **1-Cs** is very similar to that of **3-Cs** with the only difference of partial (1/12) substitution of W by Cu and partial (11/12) occupancy of terminal O. W, O, P and Cs atoms are shown in grey, red, purple and green spheres, respectively.

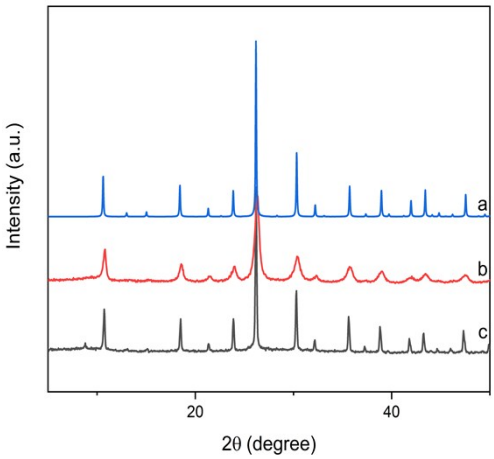

Fig. S5 Simulated powder XRD pattern of **3-Cs** (a), experimental powder XRD patterns of **3-Cs** (b) and **1-Cs** (c).

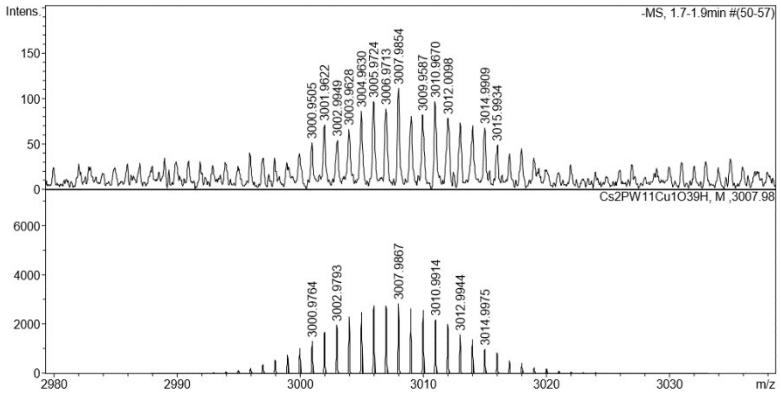

Fig. S6 The experimental (above) and simulated (below) ESI-MS peak of $[Cs_2HCuPW_{11}O_{39}]^-$.

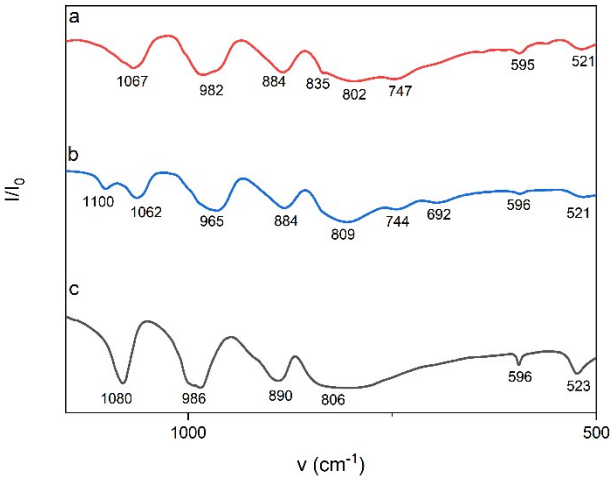

Fig. S7 IR spectra of **1-Cs** (a), **2-Cs** (b) and **3-Cs** (c) in the range of 1150~500 cm^{-1}.

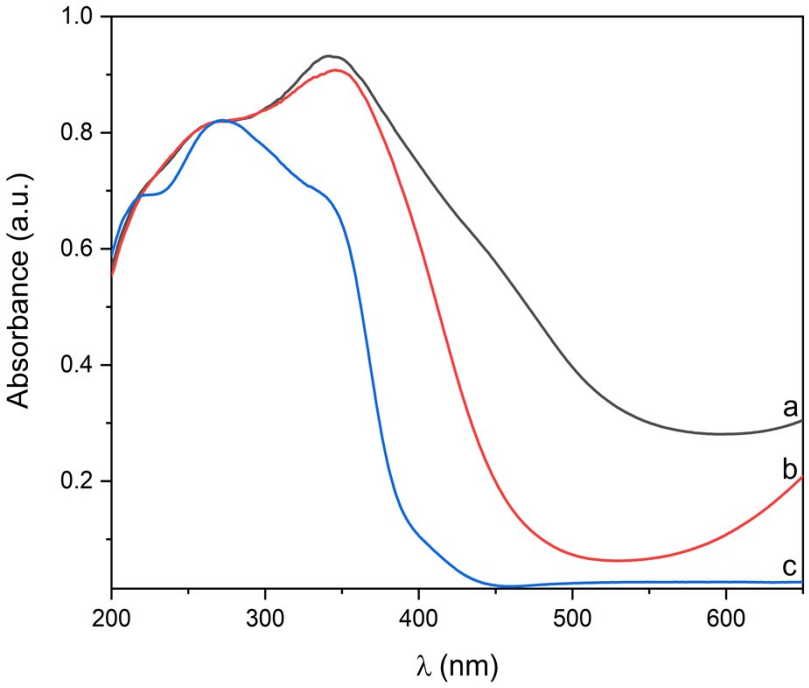

Fig. S8 UV-Vis diffuse reflectance spectra of **1-Cs** (a), **2-Cs** (b) and **3-Cs** (c).

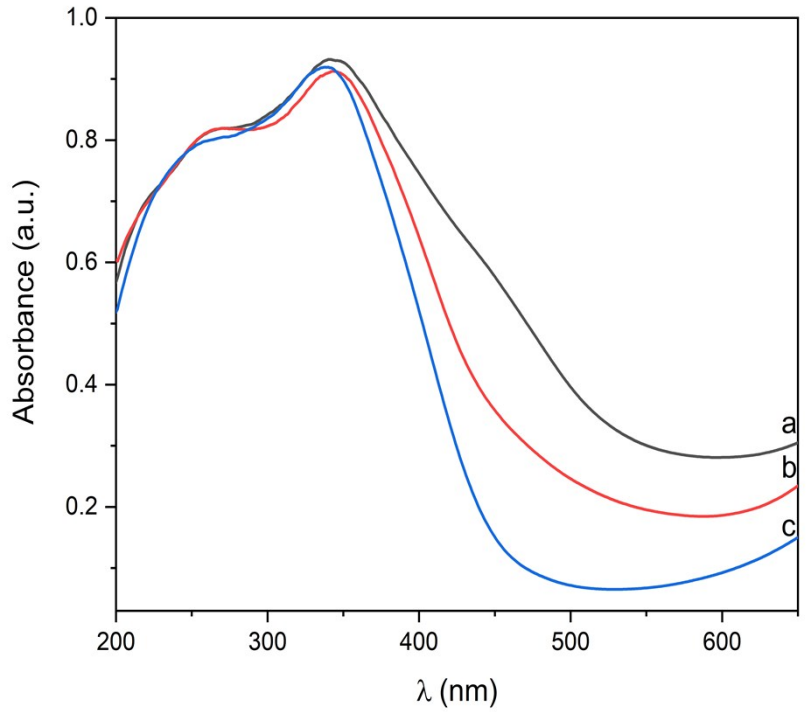

Fig. S9 UV-Vis diffuse reflectance spectra of **1-Cs** after 0 (a), 4 (b) and 9 (c) day(s).

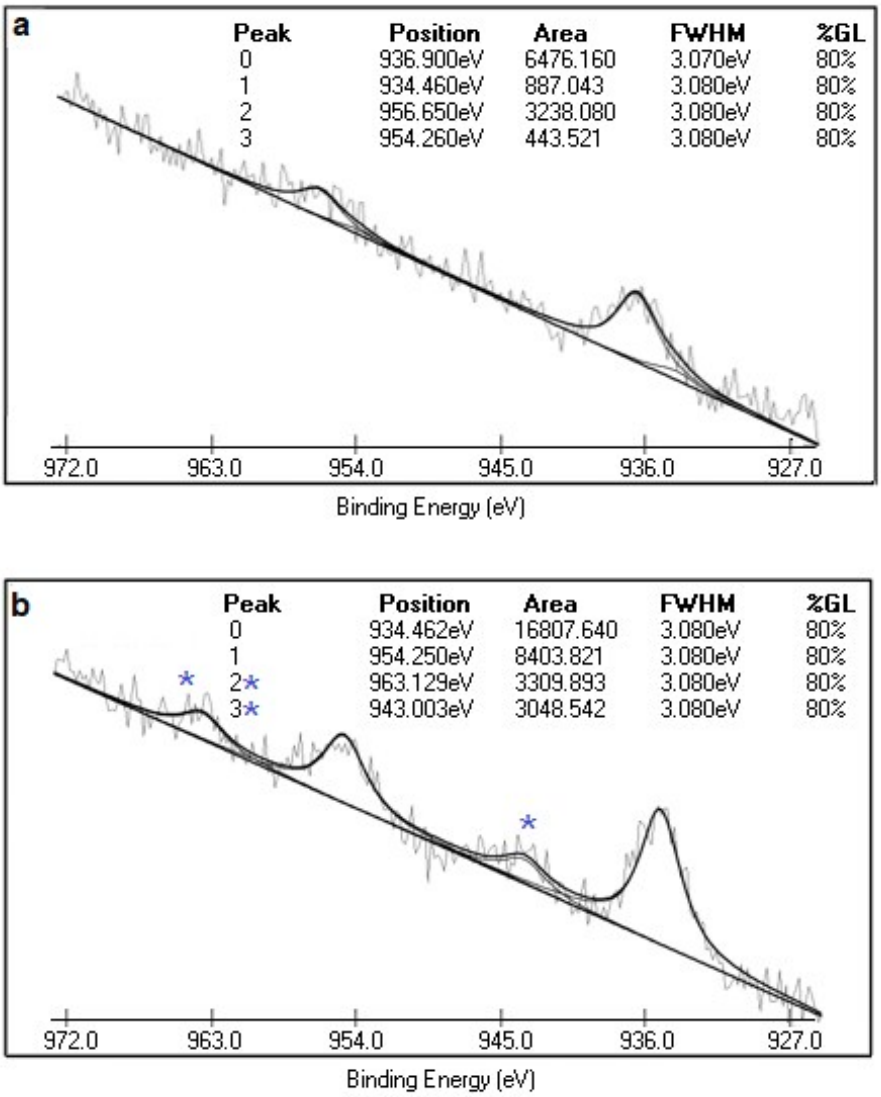

Fig. S10 Cu 2p XPS spectra of **1-Cs** (a) and **2-Cs** (b). Peaks marked with asterisks represent satellite peaks of Cu^{2+}.

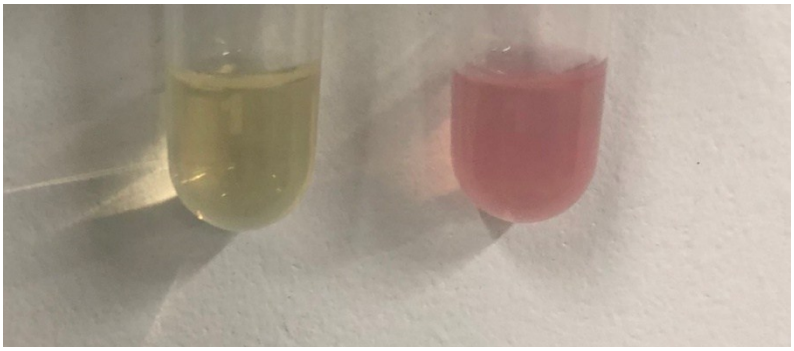

Fig. S11 Solution of $Na_5[Mn^{II}PW_{11}O_{39}(OH_2)]\cdot 15H_2O$ after mixed with **2-Cs** (left) and **1-Cs** (right) followed with filtering.

Reference:

A1. G. M. Brown, M. R. Noe-Spirlet, W. R. Busing and H. A. Levy, *Acta Crystallogr. B*, 1977, **33**, 1038-1046.

A2. J. A. Santos, *Proc. Roy. Soc. A*, 1935, **150**, 309-322.